

1 **Demographic signals of population decline and time to**  
2 **extinction in a seasonal, density-dependent model**

3 Joseph B. Burant<sup>1,2,\*</sup> and D. Ryan Norris<sup>1</sup>

4 **Author affiliations:**

5 <sup>1</sup> Department of Integrative Biology, University of Guelph, Guelph, Ontario, Canada, N1G 2W1

6 <sup>2</sup> Current address: Department of Animal Ecology, Netherlands Institute of Ecology, 6708 PB

7 Wageningen, Netherlands

8 **ORCID accounts:**

9 JBB: <https://orcid.org/0000-0002-0713-3100>

10 DRN: <https://orcid.org/0000-0003-4874-1425>

11 \* **Corresponding author:** j.burant@nioo.knaw.nl

12 **Acknowledgements**

13 This research was funded by a Discovery Grant to DRN from the Natural Sciences and  
14 Engineering Research Council of Canada. JBB was supported by an Ontario Graduate  
15 Scholarship and Queen Elizabeth II Graduate Scholarship in Science and Technology from the  
16 Ontario Government and a Graduate Tuition Scholarship from the University of Guelph.

17

18 **Declarations**

19 **Funding:** Natural Sciences and Engineering Research Council of Canada; Government of  
20 Ontario; University of Guelph

21 **Conflicts of interest:** The author declare no competing interests.

22 **Availability of data and material:** The simulated data used in the analyses have been made  
23 available on Figshare: <https://doi.org/10.6084/m9.figshare.14515194> (Burant and Norris 2023).

24 **Code availability:** The code for the theoretical model is publicly available on Figshare:  
25 <https://doi.org/10.6084/m9.figshare.14515194> (Burant and Norris 2023).

26 **Author contributions:** Both authors were involved in initial discussions to develop the  
27 theoretical population model. JBB constructed the model, performed the analyses, and wrote the  
28 first draft. Both authors revised the manuscript for publication.

29 **Ethics approval:** Not applicable.

30 **Consent to participate:** Not applicable.

31 **Consent to publication:** Not applicable.

32 **Manuscript summary:**

33 Abstract word count: 251 words

34 Main text word count (excluding abstract, reference list, figure captions): 5,954 words

35 Number of figures: 5

36 Number of tables: 0

37 Number of references: 69

38 Number of supplementary items: 6

39 **Abstract**

40 Nearly all wild populations live in seasonal environments in which they experience regular  
41 fluctuations in environmental conditions that drive population dynamics. Recent empirical  
42 evidence from experimental populations of *Drosophila* suggests that demographic signals  
43 inherent in the counts of seasonal populations, including reproduction and survival, can indicate  
44 when in the annual cycle habitat loss occurred. However, it remains unclear whether these  
45 signatures of season-specific decline are detectable under a wider range of demographic  
46 conditions and rates of habitat loss. Here, we use a bi-seasonal Ricker model to examine season-  
47 specific signals of population decline induced by different rates of habitat loss in the breeding or  
48 non-breeding season and different strengths of density dependence. Consistent with the findings  
49 in *Drosophila*, breeding habitat loss was accompanied by reduced reproductive output and a  
50 density-dependent increase in survival during the subsequent non-breeding period. Non-breeding  
51 habitat loss resulted in reduced non-breeding survival and a density-dependent increase in  
52 reproduction in the following breeding season. These season-specific demographic signals of  
53 decline were present under a wide range of habitat loss rates (2-25% per generation) and  
54 different density-dependent regimes (weak, moderate, and strong). We show that stronger  
55 density dependence can negatively influence time to extinction when non-breeding habitat is  
56 lost, whereas the strength of density dependence does not influence time to extinction with  
57 breeding habitat loss (although, in all cases, density dependence itself was an important  
58 modulator of population dynamics). Our results illustrate the need to incorporate seasonality in  
59 theoretical models to better understand when populations are being driven to decline.

60 **Keywords:** bi-seasonal, breeding, carrying capacity, density dependence, extinction, non-  
61 breeding, Ricker model, vital rates

## 62 **Introduction**

63 Habitat loss and fragmentation due to human land-use, have been identified as the leading causes  
64 of decline in wild populations observed in recent decades (Pimm et al. 2014; Díaz et al. 2019;  
65 but see Fahrig 2003, 2019). Habitat deterioration is the primary risk to approximately 30 percent  
66 of threatened species and one of the major threats to 85 percent of all species identified on the  
67 IUCN's Red List (World Wildlife Fund 2018; Intergovernmental Science-Policy Platform on  
68 Biodiversity and Ecosystem Services 2019). An understanding of not only what environmental  
69 factors are driving these populations to extinction, but also when and where these forces play out  
70 within the annual cycle, is imperative to global conservation efforts. Simple demographic models  
71 provide a theoretical underpinning to our understanding of the dynamics of natural systems, and  
72 represent an important tool in our arsenal for characterizing, managing, and conserving  
73 threatened populations (Beissinger and Westphal 1998; Gimona 1999; Norris 2004; García-Díaz  
74 et al. 2019).

75         Climatic seasonality is a fundamental component of natural environments, driving the  
76 regular fluctuations in resource availability and quality to which most species and populations  
77 are subjected. And yet, early models of population growth, such as the logistic growth curve  
78 (Verhulst 1845; Pearl and Reed 1920) and the Ricker model (Ricker 1954) did not explicitly  
79 incorporate the potential for seasonal dependence, and the population dynamical implications of  
80 seasonality are generally underappreciated (White and Hastings 2020). Despite their simplicity,  
81 these models can still offer important insights into fundamental ecological processes that  
82 underpin the dynamics of a wide range of natural systems (Ricker 1963; Borlestean et al. 2015;  
83 Romero et al. 2017; Bolser et al. 2018). Although population models are still frequently framed  
84 around a stationary, or 'aseasonal', context (Ludwig 1996; Mueller and Joshi 2000; Lande et al.  
85 2003; Otso and Meerson 2010), explicit incorporation of the impacts of seasonality on  
86 population dynamics has proven fruitful (Skellam 1967; Fretwell 1972; Kot and Schaffer 1984;  
87 Sutherland 1996; Norris 2005; Liz 2017).

88         Despite lacking explicit seasonality, the strength of simple population models like the  
89 logistic and Ricker models is that they capture the important role of density dependence in  
90 explaining fluctuations in abundance over time. Density-dependent mechanisms arise when the  
91 rate of population growth (or change) at any given time is, at least in part, contingent on the  
92 current population density (Hassell 1986). The strength of density dependence is expected to

93 modulate the effects of habitat loss and impact population responses to environmental change  
94 (Sutherland 1996; Agrawal et al. 2004; Norris 2005). Sequential density dependence, through  
95 which population abundance in one season influences population vital rates in the next (Norris  
96 2005; Ratikainen et al. 2007; Betini et al. 2013a), may affect the capacity for populations to  
97 respond to environmental change, and may also result in different system dynamics in those  
98 losing breeding or non-breeding habitat. While aseasonal models generally capture density  
99 dependence in population growth rate ( $r$ ), seasonal models allow the decomposition of density-  
100 dependent effects in the different periods (i.e., in a bi-seasonal model, we can now model two  
101 growth rates,  $r_b$  in the breeding period and  $r_{nb}$  in the non-breeding period). In a series of studies,  
102 Betini et al. (2013a, 2013b, 2014) demonstrated how density dependence acts to regulate  
103 seasonal population dynamics in an experimental population of *Drosophila melanogaster* with  
104 distinct breeding and non-breeding periods.

105         In a recent experimental study, we investigated how seasonal changes in habitat  
106 availability influenced the dynamics of the same seasonal *Drosophila* populations, and found  
107 that populations losing breeding versus non-breeding habitat responded in the different ways  
108 (Burant et al. 2019). In the experiment, seasonality was induced by manipulating the quality food  
109 provided (Betini et al. 2013b) and chronic, season-specific habitat loss was imposed over  
110 multiple generations by systematically reducing the volume of food provide in one period while  
111 holding it constant in the other (Burant et al. 2021). The loss of breeding habitat resulted in a  
112 decline in *per capita* reproduction and, as a consequence of fewer individuals entering the  
113 subsequent non-breeding period, an increase in non-breeding survival via positive sequential  
114 density dependence. Conversely, loss of non-breeding habitat had the opposite effect: non-  
115 breeding survival declined due to resource limitation, while *per capita* reproduction showed an  
116 increase in the subsequent breeding period via positive sequential density dependence (Burant et  
117 al. 2019). Moreover, we demonstrated that simple demographic and statistical signals derived  
118 from population counts and vital rates, including non-breeding survival, reproduction and other  
119 statistical indicators inherent in time series of population abundance, can be used to identify the  
120 season in which habitat loss occurred (Burant et al. 2019). However, the experiment only  
121 considered two different rates of breeding or non-breeding habitat loss (10% and 20% per  
122 generation) and was conducted under levels of breeding and non-breeding density dependence  
123 characteristic of a specific, laboratory-evolved strain of *Drosophila*. Thus, the extent to which

124 these empirical results are relevant for other populations under a broader range of strengths of  
125 density dependence and rates of habitat loss remains unclear.

126         In this study, we use a bi-seasonal Ricker model (Betini et al. 2013a) to explore how  
127 different rates of habitat loss in either the breeding or non-breeding period and the strength  
128 density dependence influence the production of simple, season-specific signals of population  
129 decline and time to extinction *in silico*. The original (aseasonal) Ricker model was developed in  
130 the context of fisheries harvesting (Ricker 1954) and has since been extended for application in a  
131 variety of contexts, modelling the population dynamics for a broad range of taxa, including  
132 fishes (e.g., Myers et al. 1999), crustaceans (e.g., Twombly et al. 2007), and insects (e.g., Dey  
133 and Joshi 2006; Estay et al. 2009). Here, we incorporate the effects of season-specific habitat  
134 loss on carrying capacity and growth in each period of the bi-seasonal model, and use  
135 simulations to explore how habitat loss operates under a range of initial parameter values,  
136 strengths of density dependence, and rates of seasonal habitat loss. We derive season-specific  
137 vital rates (survival and reproduction) to look at sequential density-dependence between periods  
138 of breeding and non-breeding (Betini et al. 2013a), rather than density dependence in population  
139 growth between generations.

140         Given the discrete nature of our model, with breeding and non-breeding conditions  
141 modelled as two separate equations and resource pools (habitats), we expect that this model may  
142 be particularly relevant for migratory species (e.g., migratory birds) that occupy distinct breeding  
143 and non-breeding habitats. For example, our model captures the plausible scenario in which a  
144 population experiences habitat loss (or another environmental forcing) on the breeding grounds,  
145 while the non-breeding sites remain relatively stable (or *vice versa*). However, even in resident  
146 species that occupy the same habitat throughout the year, populations may experience  
147 differential changes in resource availability and quality during periods of breeding and non-  
148 breeding, which may impact their overall dynamics in a similar way. Thus, the model we present  
149 and others that explicitly incorporate seasonality (White and Hastings 2020) have a broad scope  
150 of application.

151 **Methods**152 *Bi-seasonal Ricker model with season-specific habitat loss*

153 The Ricker model (eq. 1) was first introduced by W.E. Ricker (1954) in the context of fisheries  
 154 management, following his observation that the convex relationship between net reproduction  
 155 and population density resulted in oscillations in population abundance. Since then, the Ricker  
 156 model has become one of the classical theoretic models to describe density-dependent dynamics  
 157 in populations with discrete time intervals (Fretwell 1972; Kot and Schaffer 1984; Turchin 2003;  
 158 Geritz and Kisdi 2004; Wysham and Hastings 2008). The Ricker model can be expressed as:

$$N_{(t+1)} = N_{(t)} e^{r \left(1 - \frac{N_{(t)}}{K}\right)} \quad (\text{eq. 1})$$

159 where  $N$  represents the number of individuals in the population at a given time  $t$ ,  $r$  is the intrinsic  
 160 growth rate ('Malthusian parameter'; Fisher 1930), and  $K$  indicates a population's carrying  
 161 capacity (Pearl and Reed 1920). The simple Ricker model has been used previously to model the  
 162 population dynamics of *Drosophila* (Mueller and Joshi 2000; Dey and Joshi 2006). This  
 163 aseasonal model results in stable population cycles for a range of  $r$  and  $K$ , which can be either  
 164 arbitrary or empirically defined, but generates chaotic dynamics when  $r$  is large ( $r > \sim 2.7$ ; May  
 165 and Oster 1976; May 1987). Griffen and Drake (2008) showed that reductions in habitat quality  
 166 produced reductions in both  $r$  and  $K$ , as modelled for experimental populations of the water flea  
 167 *Daphnia magna*.

168 To investigate the dynamics of *D. melanogaster* with distinct breeding and non-breeding  
 169 periods, Betini et al. (2013a) extended the Ricker model to include season-specific parameters  
 170 for population growth and carry capacity. For this 'seasonal' Ricker model, temporal changes in  
 171 breeding ( $N_b$ ) and non-breeding ( $N_{nb}$ ) population abundance can be modelled using a set of two  
 172 interacting equations (eq. 2.1, 2.2). For each generation, population size at the beginning of the  
 173 non-breeding period (i.e., the number of offspring produced; maximum population size in a  
 174 given generation) can be written as the difference equation:

$$N_{nb(t+1)} = N_{b(t)} e^{r_b \left(1 - \frac{N_{b(t)}}{K_b}\right)} \quad (\text{eq. 2.1})$$

175 where  $r_b$  and  $K_b$  are the maximum growth rate (reproduction) and carrying capacity for the  
 176 breeding period,  $b$ , respectively. In this way, nonbreeding,  $nb$ , population size ( $N_{nb}$ ) is a product  
 177 of the number of breeders ( $N_b$ ) and density-dependent interactions between them (Betini et al.

178 2013a, 2013b). Population size at the beginning of the breeding period (i.e., the number of  
 179 potentially breeding adults that survived the previous non-breeding period) can be described as:

$$N_{b(t+1)} = N_{nb(t+1)} e^{r_{nb} \left(1 - \frac{N_{nb(t+1)}}{K_{nb}}\right)} \quad (\text{eq. 2.2})$$

180 where  $r_{nb}$  and  $K_{nb}$  are the maximum growth rate (mortality) and carrying capacity for the non-  
 181 breeding period, respectively.

182 In this study, we were interested in modelling the impacts of chronic, season-specific  
 183 habitat loss on the predicted changes in breeding and non-breeding population size under a range  
 184 of conditions. In a previous experiment (Burant et al. 2019), we systemically reduced the amount  
 185 of food provided to replicate populations of *Drosophila* in either the breeding or non-breeding  
 186 period over multiple generations, until the populations went extinct. In our experiment, and in  
 187 the theoretical model presented here, season-specific habitat loss followed an exponential decay,  
 188 with the proportion of food provisioned in the season of habitat loss in a particular generation  
 189  $H_{(t)}$  prescribed as:

$$H_{(t)} = (1 - v)^t \quad (\text{eq. 3})$$

190 where  $v$  is the rate of habitat loss and  $t$  is the number of generations since habitat loss treatment  
 191 commenced.

192 In an attempt to replicate the experimental reductions in habitat, we represented habitat  
 193 loss by altering season-specific  $r$  and  $K$  parameters. Given that both population growth rate and  
 194 carrying capacity have been shown to be dependent on the quantity of food provisioned (Griffen  
 195 and Drake 2008), we scaled both parameter values proportionally with the rate of habitat loss.  
 196 For populations losing breeding habitat, our model assumed that both  $r_b$  and  $K_b$  would decrease  
 197 proportionally with the rate of habitat loss (eq. 4.1), such that the total number of offspring  
 198 produced by the previous generation  $N_{nb(t+1)}$  would also decrease. Changes in population growth  
 199 rates and carrying capacities with breeding habitat loss can be summarized as:

$$K_{b(t)} = K_b^* H_{b(t)} \quad (\text{eq. 4.1})$$

$$r_{b(t)} = r_b^* - r_b^* (1 - H_{b(t)}) = r_b^* H_{b(t)}$$

$$K_{nb(t)} = K_{nb}^*$$



$$r_{nb(t)} = r_{nb}^*$$

200 where  $K_b^*$  and  $r_b^*$  are the estimated carrying capacity and intrinsic growth rate during the  
 201 breeding period under control (no habitat loss) conditions, respectively,  $K_{nb}^*$  and  $r_{nb}^*$  are the  
 202 corresponding non-breeding values, and  $H_{b(t)}$  is the proportion of breeding habitat remaining.

203 For populations losing non-breeding habitat, we expected the opposite effects on season-  
 204 specific growth rates and carrying capacities. We predicted that  $K_{nb}$  would decrease  
 205 proportionally to the rate of habitat loss and  $r_{nb}$  would become more negative (increasing  
 206 mortality) as the proportion of habitat remaining continued to decline (eq. 4.2). Changes in  
 207 population growth rates and carrying capacities with non-breeding habitat loss can be  
 208 summarized as:

$$K_{b(t)} = K_b^* \tag{eq. 4.2}$$

$$r_{b(t)} = r_b^*$$

$$K_{nb(t)} = K_{nb}^* H_{nb(t)}$$

$$r_{nb(t)} = r_{nb}^* - |r_{nb}^*|(1 - H_{nb(t)})$$

209 where  $H_{nb(t)}$  is the proportion of non-breeding habitat remaining. Scaling the season-specific  
 210 growth rates and carrying capacities in this way had the effect of holding the strength of density  
 211 dependence (see below) constant in the season of habitat loss.

### 212 *Model simulations*

213 To explore the dynamics of our bi-seasonal Ricker model with season-specific habitat loss, we  
 214 first parameterized the model using estimates derived from a set of input-output experiments in  
 215 seasonal populations of *Drosophila* (Betini et al. 2013a). In these trials, populations of breeding  
 216 and non-breeding fruit flies were initiated at a range of densities, and their subsequent  
 217 reproductive output (breeding) and survival (non-breeding) were measured. The experimental  
 218 density dependence reference parameters from Betini et al. (2013a) were:  $r_b = 2.24$ ,  $\alpha_b = 9.86 \times$   
 219  $10^{-3}$ ,  $r_{nb} = -0.0568$ , and  $\alpha_{nb} = 6.72 \times 10^{-4}$ , where  $\alpha$  describes the strength of density dependence in  
 220 an alternative form of the Ricker model and can be calculated as  $\alpha_i = r_i / K_i$  (see *Supplementary*  
 221 *Information* for results of model parameterization with empirical values; Fig. S3).

222 To investigate how the strength of density dependence influenced the trajectories of  
 223 populations and the production of seasonal signals of decline, we further explored three other  
 224 parameterizations in which the strength of density dependence was manipulated by changing the  
 225 value of  $r$  (in the same direction) in both seasons: (1) weak density dependence ( $r_b = 1.3$ ,  $r_{nb} = -$   
 226  $0.033$ ); moderate density dependence ( $r_b = 2$ ,  $r_{nb} = -0.051$ ); strong density dependence ( $r_b = 2.65$ ,  
 227  $r_{nb} = -0.069$ ). These values of  $r_b$  are selected somewhat arbitrarily to sample the range of the non-  
 228 zero equilibrium, non-chaotic phase of the Ricker model ( $r < 1$  results in populations shrinking  
 229 to zero; chaotic dynamics set in at  $r \approx 2.7$ ). The corresponding  $r_{nb}$  values are matched based on  
 230 the ratio of the experimentally-derived parameters (e.g.,  $r_{nb(moderate)} = r_{nb(experimental)} \times 2 / 2.24$ ).  
 231 This manipulation of  $r$  is consistent with previous experimental work, which has shown that,  
 232 intuitively, maximum growth rates may be useful as a predictor of the strength of density  
 233 dependence in systems that conform to the monotonic definition of density dependence inherent  
 234 in most simple population models (Agrawal et al. 2004). Because carrying capacity is largely a  
 235 function of the volume of food provided (e.g., Griffen and Blake 2018; Burant et al. 2020), and  
 236 not the strength of density dependence, the season-specific carrying capacities ( $K_b = 227$ ,  $K_{nb} = -$   
 237  $84.5$ ) were the same for all three theoretical scenarios and the initial empirical parameterization.

238 To simulate some degree of variability in the baseline parameters, which should be  
 239 expected for real world replicate populations, we treated these parameters as normal distributions  
 240  $N(\mu, \sigma^2)$  from which the initial values  $K_b^*$ ,  $r_b^*$ ,  $K_{nb}^*$ , and  $r_{nb}^*$  could be sampled. For the season-  
 241 specific carrying capacities, the standard deviation of  $K_i$  was set as  $\sqrt{|K_i|}$ . Since the square-root  
 242 of a value  $< 1$  is larger than the initial value, the standard deviation for the season-specific  
 243 growth rates  $r_i$  was set as  $r_i/10$ .

244 We simulated a range of rates of season-specific habitat loss, with populations losing  
 245 habitat at a rate of 2%, 5%, 10%, 20%, or 25% per generation in either the breeding or the non-  
 246 breeding period. We also included control simulations, in which habitat availability was constant  
 247 in both seasons. As with our experiment, which included 10% and 20% rates of habitat loss  
 248 (Burant et al. 2019), replicate simulations were initiated with a non-breeding population size of  
 249 20 individuals. We simulated 20 generations of ‘pre-treatment’ population growth in which the  
 250 proportion of habitat provisioned in the treatment period remained at 100%. Starting in  
 251 generation 21, the simulated proportion of habitat provisioned in the treatment period

252 corresponded to the rate of loss following eq. 3. We ran each model simulation for 50  
 253 generations (including the pre-treatment period), or until the population went extinct.

254 For each strength of density dependence scenario, we performed 1,000 model simulations  
 255 for different rate of loss and season of loss combinations (e.g., 2% breeding, 2% non-breeding,  
 256 5% breeding, etc.), with 10 rate-by-season treatment combinations plus controls. In order to  
 257 avoid overfitting our statistical models (see *Supplementary Information*), and to introduce an  
 258 additional degree of randomness in the initial parameter values that were used to specify each  
 259 run, we randomly sampled 25 of the 1,000 simulations for each treatment for analysis.

260 From each replicate, we derived time series of the following metrics: (1) *breeding*  
 261 *abundance* (i.e., the number of potential breeders, the number of individuals at the end of the  
 262 non-breeding period); (2) *non-breeding abundance* (i.e., the number of offspring produced, the  
 263 number of individuals at the start of the non-breeding period); (3) *per capita reproduction* (i.e.,  
 264 the relative change in abundance between the beginning and end of the breeding period, non-  
 265 breeding abundance / breeding abundance); and (4) *non-breeding survival* (i.e., the relative  
 266 change in abundance between the beginning and end of the non-breeding period, breeding  
 267 abundance / non-breeding abundance). Time to extinction was calculated as the number of  
 268 generations from the initiation of habitat loss (i.e., generation – 20) until abundance  $\leq 2$   
 269 individuals in the breeding period.

#### 270 *Relative strength of density dependence*

271 To explore the density-dependent nature of time to extinction that we identified in our model  
 272 simulations of non-breeding habitat loss, we systemically varied the strength of density  
 273 dependence in either the breeding and non-breeding period independently while holding density  
 274 dependence constant (moderate) in the other season. As with all parameterizations, the relative  
 275 strength of density dependence was always higher in the breeding period ( $\alpha_{\text{weak}} = 5.73 \times 10^{-3}$ ,  
 276  $\alpha_{\text{moderate}} = 8.81 \times 10^{-3}$ ,  $\alpha_{\text{strong}} = 1.17 \times 10^{-2}$ ) than that in non-breeding period ( $\alpha_{\text{weak}} = 3.91 \times 10^{-4}$ ,  
 277  $\alpha_{\text{moderate}} = 6.00 \times 10^{-4}$ ,  $\alpha_{\text{strong}} = 8.11 \times 10^{-4}$ ; see *Model simulations*). Extinction time was  
 278 determined by performing a single iteration of the non-breeding habitat loss model with each  
 279 combination of breeding and non-breeding strengths of density dependence.

280 The theoretical model was constructed in the R statistical environment (v. 4.0.2; R Core Team  
281 2020). The code and data used in these analyses have been made publicly available (Burant and  
282 Norris 2022).

## 283 **Results**

### 284 *Bi-seasonal population dynamics with habitat loss*

285 Simulations of a bi-seasonal Ricker model with season-specific habitat loss (see *Model*  
286 *simulations* in *Methods*) produced two counts in each generation (breeding abundance and non-  
287 breeding abundance), with distinct dynamics that varied with the season and rate of habitat loss  
288 (Fig. 1). In the initial pre-treatment generations, during which all replicate populations were  
289 allowed to grow from an initial non-breeding population size of 20 individuals, all treatment  
290 scenarios showed a rapid increase towards carrying capacity and stable seasonal oscillations in  
291 the generations preceding the introduction of treatment. For control replicates, in which habitat  
292 availability remained constant in both the breeding and non-breeding period, population  
293 abundances in both seasons were stable throughout the treatment period. Control breeding  
294 abundance was largely similar across the different strengths of density dependence (mean  
295 breeding abundance: weak DD =  $206 \pm 2.48$  (mean  $\pm$  SE); moderate DD =  $200 \pm 3.89$ ; strong  
296 DD =  $199 \pm 2.51$ ; Fig. 1a, d, g; Fig. S1). In contrast, control non-breeding abundance increased  
297 with the strength of density dependence (mean non-breeding abundance: weak DD =  $233 \pm 3.20$ ;  
298 moderate DD =  $247 \pm 5.54$ ; strong DD =  $276 \pm 26.5$ ; Fig. 1a, d, g; Fig. S2). Between-season  
299 variability in abundances increased with stronger density dependence (Fig. 1).

300 With reductions in breeding habitat, there were similar patterns of decline in both  
301 breeding and non-breeding abundance, with declines in both seasons beginning within 1-2  
302 generations of the onset of treatment (Fig. 1b, e, h; Fig. S1; Fig. S2). In contrast, when non-  
303 breeding habitat was lost, breeding and non-breeding population abundance appeared to diverge  
304 in simulations (Fig. 1c, f, i; Fig. S1; Fig. S2). Breeding population abundance declined steadily  
305 as non-breeding habitat was lost, whereas non-breeding population abundance remained  
306 relatively stable for several generations before declining rapidly. At lower rates of non-breeding  
307 habitat loss (2% and 5% per generation), non-breeding abundance actually increased slightly for  
308 several generations preceding the rapid decline (Fig. 1b, e, h; Fig. S2). The transition from high,  
309 stable non-breeding abundance to rapid decline occurs around generation 21, 16, 14, 12, and 11

310 for non-breeding habitat loss treatments of 2%, 5%, 10%, 20%, and 25% habitat loss per  
311 generation (Fig. S3).

### 312 *Response of vital rates to season-specific habitat loss*

313 As expected, breeding and non-breeding habitat loss generated distinct changes in population  
314 vital rates (Fig. 2; Fig. 3; *Supplementary Information*). For control replicates, *per capita*  
315 reproduction declined rapidly as populations grew towards carrying capacity in the pre-treatment  
316 period, and remained stable during the treatment generations (mean *per capita* reproduction =  
317  $1.13 \pm 0.004$ ,  $1.28 \pm 0.04$ , and  $2.07 \pm 0.40$  offspring/breeder with weak, moderate, and strong  
318 density dependence, respectively; Fig. 2a, d, g). When breeding habitat was lost, *per capita*  
319 reproduction dropped and remained below one (i.e., the replacement value) as the amount of  
320 breeding habitat available in each generation continued to decline. *Per capita* reproduction  
321 shifted from being relatively stable in the generations preceding population collapse to zero  
322 within a single generation (Fig. 2b, e, h). In contrast, non-breeding habitat loss generated a  
323 steady increase in *per capita* reproduction, with values exceeding those observed for control  
324 simulations, as one might expect given the assumed pattern of compensatory density dependence  
325 (Fig. 2c, f, i). As the rate of non-breeding habitat loss increased, the relative increase in *per*  
326 *capita* reproduction decreased, likely as a result of reduced time available for simulations to  
327 respond to shifting conditions.

328 Non-breeding survival remained relatively high throughout the treatment period for control  
329 simulations (mean non-breeding survival =  $88.4 \pm 0.003\%$ ,  $79.1 \pm 0.006\%$ , and  $75.7 \pm 0.02\%$  for  
330 weak, moderate, and strong density dependence, respectively), and was as high as 100% in the  
331 initial generations of the pre-treatment period (Fig. 3a, d, g). When breeding habitat was lost, the  
332 proportion of individuals that survived the non-breeding period increased to one as the number of  
333 individuals entering the non-breeding period decreased (Fig. 3b, e, h). With non-breeding habitat  
334 loss, non-breeding survival decreased proportionally with the rate of habitat loss (Fig. 3c, f, i).  
335 Interestingly, all non-breeding habitat loss simulations reached a plateau around 20-25% non-  
336 breeding survival in later generations (i.e., when the volume of non-breeding habitat provisioned  
337 was low), with non-breeding survival actually increasing in the generation preceding population  
338 collapse, before declining to zero as the populations went extinct. This result may provide some

339 evidence for an Allee effect on survival with non-breeding habitat loss, likely because relatively  
340 few offspring are produced by breeders at very low densities.

341 *Time to extinction*

342 Season-specific habitat loss resulted in rapid changes in bi-seasonal population dynamics, with  
343 breeding and non-breeding habitat loss generating different patterns of population decline and  
344 timing of population collapse (Fig. 1b, c, e, f, h, i). As expected, the pace at which populations  
345 declined towards extinction increased with the rate of habitat loss. However, there was a notable  
346 difference between simulations of breeding and non-breeding habitat loss in the effect of the  
347 strength of density dependence on the timing of population collapse (Fig. 4). When breeding  
348 habitat was lost, the timing of population collapse appeared to be almost entirely dependent on  
349 the rate of habitat loss, with relatively little impact of the strength of density dependence  
350 imposed on the population (Fig. 4a). With breeding habitat loss, all replicate populations went  
351 extinct within 19, 11, 7, 4, and 3 generations with the onset of habitat loss treatments of 2%, 5%,  
352 10%, 20%, and 25% loss per generation, respectively. In contrast, when non-breeding habitat  
353 was lost, the time to extinction was negatively related to the strength of density dependence (Fig.  
354 4b), such that populations subjected to weak density dependence collapsed later than those  
355 subjected to strong density dependence. Across all scenarios, populations losing non-breeding  
356 habitat went extinct earlier than those losing breeding habitat (Fig. 1; Fig. 4; Fig. S3).

357         Because we varied the strength of density dependence simultaneously in both seasons, we  
358 were also interested in examining whether season-specific variation in density dependence could  
359 be driving the negative relationship between density dependence and time to extinction when  
360 non-breeding habitat was lost. To do this, for the non-breeding habitat loss scenarios, we varied  
361 the strength of density dependence in one period while holding the other at a moderate level, and  
362 then examined the time to extinction. When the strength of non-breeding density dependence  
363 was held at a moderate level and non-breeding habitat was lost, stronger breeding density  
364 dependence resulted in earlier population extinction (Fig. 5a), similar to the results reported  
365 above. In contrast, when breeding density dependence was held at a moderate level and non-  
366 breeding habitat was lost, variation in the strength of non-breeding density dependence had no  
367 impact on the timing of population collapse (Fig. 5b).

368 **Discussion**

369 We were interested in exploring whether season-specific signals of population decline observed  
370 in earlier experiments on seasonal populations of *Drosophila* (Burant et al. 2019) arise under a  
371 wider range of demographic conditions and rates of habitat loss. Several broad similarities in the  
372 overall patterns of decline from our experiment and theoretical model suggest that the latter does  
373 a reasonable job of approximating the former. First, while mean extinction times estimated from  
374 the model (see *Bi-seasonal population dynamics with habitat loss* in *Results*) were earlier than  
375 experimentally-induced collapses (average times to extinction with 10% and 20% habitat loss per  
376 generation were 14 and 7 generations for breeding treatments, and 14 and 8 generations for non-  
377 breeding treatments; Burant et al. 2019), the relative order in extinction of populations losing  
378 breeding and non-breeding habitat was consistent with experimental observations. Likewise, in  
379 both the experiment and the model presented here, non-breeding habitat loss produced large  
380 fluctuations between breeding and non-breeding population abundance (as a result of density-  
381 dependent reproduction), while breeding habitat loss resulted in consistent, directional decline  
382 (compare Fig. 1 herein with Figure 2 in Burant et al. (2019)). While seasonality has been  
383 explicitly incorporated in other theoretical approaches (reviewed in White and Hastings 2020),  
384 and the consequences of season-specific forcing for population dynamics have also been  
385 explored (e.g., Norris 2005), here we further show how season-specific vital rates can serve to  
386 indicate the season of decline.

387 Our theoretical results demonstrate the important role that the strength of density  
388 dependence plays in determining how populations decline with seasonal habitat loss. Based on  
389 our simulations, the timing of population collapse with habitat deterioration during the breeding  
390 period was almost entirely dependent on the rate at which habitat was lost, with no impact of  
391 changes in the strength of density dependence. In contrast, strong density dependence amplified  
392 the impacts of non-breeding habitat loss, such that increased density dependence resulted in  
393 steeper population declines and earlier extinctions. The difference in the influence of density  
394 dependence with season-specific habitat loss is consistent with our predictions, and is ultimately  
395 a reflection of differences in the capacity of populations to respond to habitat loss in either the  
396 breeding or non-breeding period. With non-breeding habitat loss, populations may experience a  
397 'seasonal compensation effect' (Norris 2005) that results in increased reproduction in the  
398 subsequent breeding period. A similar compensatory effect should not necessarily be expected

399 with breeding habitat loss, since, by definition, populations cannot grow during the subsequent  
400 non-breeding period. Moreover, any seasonal compensation effect with breeding habitat loss is  
401 constrained by ceiling effects, since the proportion of individuals that survive the non-breeding  
402 period cannot exceed 100 percent. This conclusion was supported by an exploratory analysis in  
403 which we manipulated the strength of density dependence separately in each period, which  
404 showed that changing non-breeding density dependence did not affect time to extinction when  
405 breeding density dependence was moderate.

406         Inspection of the breeding and non-breeding population abundance time series revealed a  
407 number of important differences between our theoretical and experimental results (see  
408 *Supplementary Information*). First, while the relative (but not absolute) timing of collapse was  
409 consistent between the experiment and model (see above), the way in which these declines  
410 unfolded differed. Although experimental populations did not appear to respond immediately to  
411 breeding habitat loss, with population size remaining relatively stable for several generations  
412 before declining precipitously (largely due to stable breeding abundances resulting from the  
413 strong filter of the non-breeding period; Burant et al. 2019), our theoretical model generated  
414 steady declines in abundance in both seasons with the onset of breeding habitat loss. Non-  
415 breeding habitat loss had similar effects on seasonal abundances, with delayed declines in non-  
416 breeding population size relative to breeding (as a result of density-dependent reproduction;  
417 Burant et al. 2019). Despite the fact that the control conditions in the experimental seasonal  
418 *Drosophila* system were empirically derived (G.S. Betini and D.R.N., *unpublished data*), it is  
419 possible that initial breeding food availability in our experiments was in excess of what was  
420 required to maintain stable bi-seasonal dynamics. This could have resulted in a delayed  
421 population response to reductions in breeding habitat. Moreover, carrying capacity in either  
422 season is not solely a function of the volume of food provided, since there is only so much space  
423 the flies can occupy in a closed system, and so there is the potential for overcrowding (rather  
424 than absolute food availability) to limit food access and ultimately affect differences in survival  
425 and reproduction (Burant et al. 2020; Kilgour et al. 2020). The potential for overcrowding was  
426 not accounted for in our theoretical model, and so changes in carrying capacity were assumed to  
427 be simply a function of food availability (see *Methods*). As a consequence of these intricacies,  
428 relative to our experiment (Burant et al. 2019), the simple theoretical model generally



429 underestimated breeding and non-breeding population abundance with breeding habitat loss, and  
430 overestimated breeding abundance when non-breeding habitat was lost.

431 We noted that, for non-breeding habitat loss simulations, non-breeding survival appeared  
432 to temporarily plateau in later generations when little non-breeding habitat remains and, in some  
433 instances, briefly increased in the generation preceding extinction (Fig. 3c, f, i). While not  
434 specifically encoded in the model, this is reminiscent of an Allee effect (Allee 1927; Stephens et  
435 al. 1999) in which population growth is limited at low breeding densities. In essence, low non-  
436 breeding habitat availability means only a few individuals survive to the next breeding period  
437 and, as a result, reproductive output and population growth are reduced due to low densities. In  
438 turn, only a few individuals enter the subsequent non-breeding period, where habitat availability  
439 continues to decline. Thus, non-breeding densities may be better matched to habitat availability  
440 than in previous generations when non-breeding survival declined rapidly due to the breeding  
441 season density-dependent, rebound-induced mismatch between the number of individuals  
442 entering the non-breeding period and the declining habitat availability. This plateau means  
443 populations persist longer than might otherwise be anticipated based on the steep decline in non-  
444 breeding survival observed at earlier timepoints. Why this arises in our model is not necessarily  
445 intuitive, but is possibly a product of the interplay between the density-dependent  $r_b$  (stable) and  
446  $r_{nb}$  (increasingly negative). Allee effects have been explicitly incorporated in other modifications  
447 of the Ricker model (Elaydi and Sacker 2009), including the periodic Ricker map (Sacker 2006).

448 There are several other potential explanations for discrepancies between our previous  
449 observational results and theoretical outcomes. Betini et al. (2013a) showed that sequential  
450 density dependence and carry-over effects between seasons can influence reproductive output  
451 and regulate population abundance. However, fluctuations in population density and food  
452 availability between seasons are also expected to influence other aspects of individual and  
453 population performance, which may help to buffer populations against deteriorating  
454 environmental conditions. For example, reproductive output is known to be influenced by  
455 individual body condition, such that individuals who enter the breeding period in poor condition  
456 produce fewer offspring (Betini et al. 2014), and non-breeding food availability carries over to  
457 indirectly influence reproductive performance (Burant et al. 2020). These phenotypic traits, and  
458 their changes in response to seasonal variation, effectively link environmental conditions in one  
459 season with individual performance in the next (O'Connor et al. 2014). Similarly, interactions

460 among individuals in a population can be density-mediated, with individual behavioural  
461 expression modulated by social context (Sokolowski et al. 1997; Kilgour et al. 2018;  
462 Leatherbury and Travis 2019). Importantly, the impacts of density-dependent changes on  
463 population growth and individual traits are not necessarily immediately observable (Ratikainen  
464 et al. 2007). These are but a few examples of the mechanisms through which individuals and  
465 populations can respond to changing environmental conditions (Colchero et al. 2018). Although  
466 the purpose of simple population models is not necessarily to reproduce all possible mechanisms  
467 of change, discrepancies between our theoretical and empirical results demonstrate the  
468 importance of carry-over effects and other non-abundance traits that are expected to shift as the  
469 environment deteriorates. Indeed, recent theoretical work has demonstrated the importance of  
470 considering the impacts of seasonal carry-over effects on individual performance and, ultimately,  
471 how these effects scale up to influence population vital rates (e.g., Liz and Ruiz-Herrera 2016).  
472 Failure to fully consider carry-over effects is likely to limit our understanding of the dynamics of  
473 declining populations, and so also limit efforts to conserve them (O'Connor and Cooke 2015).

474         The present model is not the first to consider how seasonality shapes the dynamics of  
475 animal populations. Fretwell (1972) expounded at length about the various ways regularly  
476 varying environments influences individual reproduction and survival and, ultimately, population  
477 persistence. Others have considered the more general case of resource variability across different  
478 temporal scales (e.g., Hastings 2014). In its original formulation, the bi-seasonal Ricker model  
479 from Betini et al. (2013a) was important for demonstrating how explicit incorporation of density-  
480 mediated carry-over effects better captures long-term vital rate dynamics and population  
481 stability. The interplay between seasonality and stability was also explored by Kot and Schaffer  
482 (1984), who showed theoretically how moderate seasonality may stabilize populations in  
483 productive environments. Consistent with our findings, Kot and Schaffer (1984) also showed  
484 how increasing 'imbalance' between breeding and non-breeding seasons periods can have  
485 contrasting effects. Sutherland (1996) more explicitly considered the effects of season-specific  
486 habitat loss on the dynamics of migratory populations, and similarly found differential effects of  
487 breeding and non-breeding habitat loss. Although time to extinction was not directly evaluated,  
488 Sutherland (1996) showed that, compared to breeding habitat loss, the same amount of non-  
489 breeding habitat loss had more than twice the effect in terms of percent population decline. This  
490 is consistent with our finding that populations losing non-breeding habitat go extinct earlier than

491 those losing breeding habitat. Our analysis complements these previous studies by showing how  
492 sequential density-dependent effects can modulate patterns of population decline and time to  
493 extinction with chronic, season-specific forcing. By simulating habitat deterioration in one  
494 season and holding it fixed in the other, we begin to explore how seasonal populations may be  
495 temporarily buffered against decline through density-dependent survival and reproduction. In  
496 addition, while we implement a seasonal formulation of the Ricker model, many other simple  
497 demographic models exist and predictions from these models may differ from those presented  
498 here. Previous comparison of the utility of different aseasonal models for predicting extinction in  
499 a community context has shown that the strong density dependence inherent in the Ricker model  
500 best matched results from simple microcosms (Ferguson and Ponciano 2013). Finally, although  
501 we randomly sampled the initial values of  $r$  and  $K$  for the iterations of each scenario, our model  
502 is strictly deterministic in that it does not incorporate a “noise” or error term, which may have  
503 implications for the interpretation of the results. Indeed, previous work has shown that  
504 incorporating demographic stochasticity can affect the reliability of extinction risk predictions  
505 drawn from simple demographic models (e.g., Drake 2005).

506         Along with understanding the demographic mechanisms underlying patterns of  
507 population decline, it is relevant to consider whether the predictability of collapse differs  
508 between populations losing breeding and non-breeding habitat. In our chronic habitat loss  
509 experiment, we showed that whether a set of indicators derived from time series of population  
510 abundance (e.g., coefficient of variation, lag-1 autocorrelation) and fitness-related traits (e.g.,  
511 body size, activity) served as early warning indicators of population collapse was dependent on  
512 the season of habitat loss (Burant et al. 2021). Moreover, in a similar theoretical approach to the  
513 one presented here, Bury (2020) showed that the nature of early warning signal production  
514 differed between simulations of breeding and non-breeding habitat degradation. This theoretical  
515 work also suggests the potential for using early warning indicators to identify the season in  
516 which populations are being driven to decline, which we also previously demonstrated in our  
517 experimental system (Burant et al. 2019). These results suggest that simple demographic vital  
518 rates like survival and reproduction, as well as early warning indicators, may be useful for  
519 detecting and predicting season-specific drivers of population decline across a wide range of  
520 density-dependent systems.

521           In summary, the results from our theoretical model of the impacts of season-specific  
522 habitat loss on population dynamics through changes in growth and carrying capacity bolster our  
523 understanding of how populations decline in seasonal environments. By comparing our  
524 theoretical simulations to results from an earlier chronic habitat loss experiment, we are able to  
525 identify some of the ways in which simple population models can elegantly capture real-world  
526 phenomena. Along with experiments and observational studies, theoretical models represent an  
527 important tool, not only for understanding how the natural world works but particularly for  
528 efforts aimed at conserving threatened species in an era of rapid environmental change.

529 **References**

- 530 Agrawal AA, Underwood N, Stinchcombe JR (2004) Intraspecific variation in the strength of  
531 density dependence in aphid populations. *Ecol Entomol* 29:521-526.  
532 <https://doi.org/10.1111/j.0307-6946.2004.00635.x>
- 533 Allee WC (1927) Animal aggregations. *Quart Rev Biol* 2:367-398.  
534 <https://doi.org/10.1086/394281>
- 535 Beissinger SR, Westphal MI (1998) On the use of demographic models of population viability in  
536 endangered species management. *J Wildl Manage* 62:821-841.  
537 <https://doi.org/10.2307/3802534>
- 538 Betini GS, Griswold CK, Norris DR (2013a) Carry-over effects, sequential density dependence  
539 and the dynamics of populations in a seasonal environment. *Proc R Soc Lond B*  
540 280:20130110. <https://doi.org/10.1098/rspb.2013.0110>
- 541 Betini GS, Griswold CK, Norris DR (2013b) Density-mediated carry-over effects explain  
542 variation in breeding output across time in a seasonal population. *Biol Lett* 9:20130582.  
543 <https://doi.org/10.1098/rsbl.2013.0582>
- 544 Betini GS, Griswold CK, Prodan L, Norris, DR (2014) Body size, carry-over effects and survival  
545 in seasonal environment: consequences for population dynamics. *J Anim Ecol* 3:1313-  
546 1321. <https://doi.org/10.1111/1365-2656.12225>
- 547 Bolser DG, Grüss A, Lopez MA, Reed EM, Mascareñas-Osorio I, Erisman BE (2018) The  
548 influence of sample distribution on growth model output for a highly exploited marine fish,  
549 the Gulf corvina (*Cynoscion othonopterus*). *PeerJ* 6:e5582.  
550 <https://doi.org/10.7717/peerj.5582>
- 551 Borlestean A, Frost PC, Murray DL (2015) A mechanistic analysis of density dependence in  
552 algal population dynamics. *Front Ecol Evol* 3:37. <https://doi.org/10.3389/fevo.2015.00037>
- 553 Burant JB, Betini GS, Norris DR (2019) Simple signals indicate which period of the annual cycle  
554 drives declines in seasonal populations. *Ecol Lett* 22:2141-2150.  
555 <https://doi.org/10.1111/ele.13393>
- 556 Burant JB, Griffin A, Betini GS, Norris DR (2020). An experimental test of the ecological  
557 mechanisms driving density-mediated carry-over effects in a seasonal population. *Can J*  
558 *Zool* 96:425-432. <https://doi.org/10.1139/cjz-2019-0271>

- 559 Burant JB, Norris, DR (2022) Code and data from: Season-specific signals of population decline  
560 and time to extinction across a broad range of conditions. Figshare.  
561 <https://doi.org/10.6084/m9.figshare.14515194>
- 562 Burant JB, Park C, Betini GS, Norris DR (2021) Early warning indicators of population collapse  
563 in a seasonal environment. *J Anim Ecol* 90:1538-1549. [https://doi.org/10.1111/1365-  
564 2656.13474](https://doi.org/10.1111/1365-2656.13474)
- 565 Bury T (2020) Detecting and distinguishing transitions in ecological systems: model and data-  
566 driven approaches. Dissertation, University of Waterloo, Waterloo
- 567 Carpenter B, Gelman A, Hoffman MD, Lee D, Goodrich B, Betancourt M, Brubaker M, Guo J,  
568 Li P, Riddell A (2017) Stan: a probabilistic programming language. *J Stat Softw* 76:1-29.  
569 <https://doi.org/10.18637/jss.v076.i01>
- 570 Colchero F, Jones OR, Conde DA, Hodgson D, Zajitschek F, Schmidt BR, Malo AF, Alberts SC,  
571 Becker PH, Bouwhuis S, Bronikowski AM, De Vleeschouwer KM, Delahay RJ,  
572 Dummermuth S, Fernández-Duque E, Frisenvænge J, Hesseilsøe M, Larson S, Lemaître J-  
573 F, McDonald J, Miller DAW, O'Donnell C, Packer C, Raboy BE, Reading CJ, Wapstra E,  
574 Weimerskirch H, While GM, Baudisch A, Flatt T, Coulson T, Gaillard, J-M (2018)  
575 Diversity of population responses to environmental change. *Ecol Lett* 22:342-353.  
576 <https://doi.org/10.1111/ele.13195>
- 577 Dey S, Joshi A (2006) Stability via asynchrony in *Drosophila* metapopulations with low  
578 migration rates. *Science* 312:434-436. <https://doi.org/10.1126/science.1125317>
- 579 Díaz S, Settele J, Brondízio ES, Ngo HT, Agard J, Arneth A, Balvanera P, Brauman KA,  
580 Butchart SHM, Chan KMA, Garibaldi LA, Ichii K, Liu J, Subramanian SM, Midgley GF,  
581 Miloslavich P, Molnár Z, Obura D, Pfaff A, Polasky S, Purvis A, Razzaque J, Reyer B,  
582 Roy Chowdhury R, Shin Y-J, Visseren-Hamakers I, Willis KJ, Zayas CN (2019) Pervasive  
583 human-driven decline of life on Earth points to the need for transformative change. *Science*  
584 266:eaax3100. <https://doi.org/10.1126/science.aax3100>
- 585 Drake JM (2005) Density-dependent demographic variation determines extinction rate of  
586 experimental populations. *PLoS Biol* 3:e222. <https://doi.org/10.1371/journal.pbio.0030222>
- 587 Elaydi SN, Sacker RJ (2009) Population models with Allee effect: a new model. *J Biol Dynam*  
588 4:397-408. <https://doi.org/10.1080/17513750903377434>

- 589 Estay SA, Lima M, Harrington R (2009) Climate mediated exogenous forcing and synchrony in  
 590 populations of the oak aphid in the UK. *Oikos* 118:175-182. [https://doi.org/10.1111/j.1600-](https://doi.org/10.1111/j.1600-0706.2008.17043.x)  
 591 [0706.2008.17043.x](https://doi.org/10.1111/j.1600-0706.2008.17043.x)
- 592 Ferguson JM, Ponciano JM (2013) Predicting the process of extinction in experimental  
 593 microcosms and accounting for interspecific interactions in single-species time series. *Ecol*  
 594 *Lett* 17:251-259. <https://doi.org/10.1111/ele.12227>
- 595 Fisher RA (1930) *The genetic theory of natural selection*. The Clarendon Press, Oxford
- 596 Fretwell SD (1972) *Populations in a seasonal environment*. Princeton University Press, Princeton
- 597 García-Díaz P, Prowser TAA, Anderson DP, Lurgi M, Binny RN, Cassey P (2019) A concise  
 598 guide to developing and using quantitative models in conservation management. *Conserv*  
 599 *Sci Practice* 1:e11. <https://doi.org/10.1111/csp2.11>
- 600 Gelman A, Goodrich B, Gabry J, Vehtari A (2018) R-squared for Bayesian regression models.  
 601 *Am Stat* 73:307-309. <https://doi.org/10.1080/00031305.2018.1549100>
- 602 Geritz SAH, Kisdi É (2004) On the mechanistic underpinning of discrete-time population models  
 603 with complex dynamics. *J Theor Biol* 228:261-269.  
 604 <https://doi.org/10.1016/j.jtbi.2004.01.003>
- 605 Gimona A (1999) Theoretical framework and practical tools for conservation o biodiversity at  
 606 the landscape scale. *Planning in Ecological Network (PLANEKO) Newsletter*, 2: 1-3.
- 607 Griffen B, Drake J (2008) Effects of habitat quality and size on extinction in experimental  
 608 populations. *Proc R Soc Lond B* 275:2251-2256. <https://doi.org/10.1098/rspb.2008.0518>
- 609 Hassell MP (1986) Detecting density dependence. *Trends Ecol Evol* 1:90-93.  
 610 [https://doi.org/10.1016/0169-5347\(86\)90031-5](https://doi.org/10.1016/0169-5347(86)90031-5)
- 611 Hastings A (2014) Temporal scales of resource variability: effects on dynamics of structured  
 612 populations. *Ecol Complex* 18:6-9. <https://doi.org/10.1016/j.ecocom.2013.08.003>
- 613 Intergovernmental Science-Policy Platform on Biodiversity and Ecosystem Services (IPBES)  
 614 (2019) *Global assessment report on biodiversity and ecosystem services*. Díaz S, Settele J,  
 615 Brondízio ES, Ngo HT, Guèze M, Argard J et al (eds). IPBES Secretariat, Bonn
- 616 Kilgour RJ, McAdam AG, Betini GS, Norris DR (2018) Experimental evidence that density  
 617 mediates negative frequency-dependent selection on aggression. *J Anim Ecol* 87:1091-  
 618 1101. <https://doi.org/10.1111/1365-2656.12813>

- 619 Kilgour RJ, McAdam AG, Norris DR (2020) Carry-over effects of resource competition and  
620 social environment on aggression. *Behav Ecol* 31:140-151.  
621 <https://doi.org/10.1093/beheco/arz170>
- 622 Kot M, Schaffer WM (1984) The effects of seasonality on discrete models of population growth.  
623 *Theor Popul Biol* 26:340-360. [https://doi.org/10.1016/0040-5809\(84\)90038-8](https://doi.org/10.1016/0040-5809(84)90038-8)
- 624 Lande R, Engen S, Sæther B-E (2003) Stochastic population dynamics in ecology and  
625 conservation. Oxford University Press, Oxford
- 626 Leatherbury KN, Travis J (2019) The effects of food level and social density on reproduction in  
627 the least killifish, *Heterandria formosa*. *Ecol Evol* 9:100-110.  
628 <https://doi.org/10.1002/ece3.4634>
- 629 Liz E (2017) Effects of strength and timing of harvest on seasonal population models: stability  
630 switches and catastrophic shifts. *Theor Ecol* 10:235-244. [https://doi.org/10.1007/s12080-](https://doi.org/10.1007/s12080-016-0325-9)  
631 [016-0325-9](https://doi.org/10.1007/s12080-016-0325-9)
- 632 Liz E, Ruiz-Herrera A (2016) Potential impact of carry-over effects in the dynamics and  
633 management of seasonal populations. *PLoS One*:e0155579.  
634 <https://doi.org/10.1371/journal.pone.0155579>
- 635 Ludwig D (1996). The distribution of population survival times. *Am Nat* 147:506-526.  
636 <https://doi.org/10.1086/285863>
- 637 May RM (1987) Chaos and the dynamics of biological populations. *Proc R Soc Lond A* 413:27-  
638 44. <https://doi.org/10.1098/rspa.1987.0098>
- 639 May RM, Oster GF (1976) Bifurcations and dynamic complexity in simple ecological models.  
640 *Am Nat* 110:573-799. <https://doi.org/10.1086/283092>
- 641 Mueller LD, Joshi A (2000). Stability in model populations. Princeton University Press,  
642 Princeton
- 643 Myers RA, Bowen KG, Barrowman NJ (1999) Maximum reproductive rate of fish at low  
644 population sizes. *Can J Fish Aquat Sci* 56:2404-2419. <https://doi.org/10.1139/f99-201>
- 645 Norris DR (2005) Carry-over effects and habitat quality in migratory populations. *Oikos*  
646 109:178-186. <https://doi.org/10.1111/j.0030-1299.2005.13671.x>
- 647 Norris DR, Taylor CM (2005) Predicting the consequences of carry-over effects for migratory  
648 populations. *Biol Lett* 2:148-151. <https://doi.org/10.1098/rsbl.2005.0397>



- 649 Norris K (2004) Managing threatened species: the ecological toolbox, evolutionary theory and  
650 declining-population paradigm. *J Appl Ecol* 41:413-426. [https://doi.org/10.1111/j.0021-](https://doi.org/10.1111/j.0021-8901.2004.00910.x)  
651 [8901.2004.00910.x](https://doi.org/10.1111/j.0021-8901.2004.00910.x)
- 652 O'Connor CM, Cooke SJ (2015) Ecological carryover effects complicate conservation. *Ambio*  
653 44:582-591. <https://doi.org/10.1007/s13280-015-0630-3>
- 654 O'Connor CM, Norris DR, Crossin GT, Cooke SJ (2014) Biological carryover effects: linking  
655 common concepts and mechanisms in ecology and evolution. *Ecosphere* 5:1-11.  
656 <https://doi.org/10.1890/ES13-00388.1>
- 657 Otso O, Meerson B (2010) Stochastic models of population extinction. *Trends Ecol Evol* 25:643-  
658 652. <https://doi.org/10.1016/j.tree.2010.07.009>
- 659 Pearl R, Reed LJ (1920) On the rate of growth of the population of the United States since 1790  
660 and its mathematical representation. *Proc Natl Acad Sci USA* 6:275-288.  
661 <https://doi.org/10.1073/pnas.6.6.275>
- 662 Pimm SL, Jenkins CN, Abell R, Brooks TM, Gittleman JL, Joppa LN, Raven PH, Roberts CM,  
663 Sexton JO (2014) The biodiversity of species and their rates of extinction, distribution, and  
664 protection. *Science* 344:1245752. <https://doi.org/10.1126/science.1246752>
- 665 Ratikainen II, Gill JA, Gunnarsson TG, Sutherland WJ, Kokko H (2007) When density  
666 dependence is not instantaneous: theoretical developments and management implications.  
667 *Ecol Lett* 11:184-198. <https://doi.org/10.1111/j.1461-0248.2007.01122.x>
- 668 R Core Team (2020) R: a language and environment for statistical computing. R Foundation for  
669 Statistical Computing, Vienna
- 670 Ricker WE (1954) Stock and recruitment. *J Fish Board Can*:559-623.  
671 <https://doi.org/10.1139/f54-039>
- 672 Ricker WE (1963) Big effects from small causes: two examples from fish population dynamics. *J*  
673 *Fish Board Can* 20:257-264. <https://doi.org/10.1139/f63-022>
- 674 Rosenblat S (1980) Population models in a periodically fluctuating environment. *J Math Biol*  
675 9:23-36. <https://doi.org/10.1007/BF00276033>
- 676 Romero MA, Grandi MF, Koen-Alonso M, Svendsen G, Ocampo Reinaldo M, García NA, Dans  
677 SL, González R, Crespo EA (2017) Analysing the natural population growth of a large  
678 marine mammal after a depletive harvest. *Sci Rep* 7:5271. [https://doi.org/10.1038/s41598-](https://doi.org/10.1038/s41598-017-05577-6)  
679 [017-05577-6](https://doi.org/10.1038/s41598-017-05577-6)

- 680 Sacker RJ (2007) A note on periodic Ricker maps. *J Differ Equ Appl* 13:89-92.  
681 <https://doi.org/10.1080/10236190601008752>
- 682 Sillett TS, Holmes RT (2005). Long-term demographic trends, limiting factors, and the strength  
683 of density dependence in a breeding population of a migratory songbird. In: Greenberg R,  
684 Marra PP (eds) *Birds of two worlds: the ecology and evolution of temperate-tropical*  
685 *migration systems*. Smithsonian Institution Press, Washington, D.C.
- 686 Skellam JG (1967) Seasonal periodicity in theoretical population ecology. *Proc 5th Berkley*  
687 *Symp Math Stat Probab* 4:179-205.
- 688 Sokolowski MB, Pereira HS, Hughes K (1997) Evolution of foraging behaviour in *Drosophila*  
689 by density-dependent selection. *Proc Natl Acad Sci USA* 94:7373-7377.  
690 <https://doi.org/10.1073/pnas.94.14.7373>
- 691 Stephens PA, Sutherland WJ, Freckleton RP (1999) What is the Allee effect? *Oikos* 87:185-190.  
692 <https://doi.org/10.2307/3547011>
- 693 Sutherland WJ (1996) Predicting the consequences of habitat loss for migratory populations.  
694 *Proc R Soc Lond B* 263:1325-1327. <https://doi.org/10.1098/rspb.1996.0194>
- 695 Turchin P (2003) *Complex population dynamics: a theoretical/empirical synthesis*. Princeton  
696 University Press, Princeton
- 697 Twombly S, Wang G, Hobbs NT (2007) Composite forces shape population dynamics of  
698 copepod crustaceans. *Ecology* 88:658-670. <https://doi.org/10.1890/06-0423>
- 699 Verhulst P-F (1845) *Recherches mathématiques sur la loi d'accroissement de la population*  
700 [French; mathematical researches into the law of population growth increase]. *Nouveaux*  
701 *Mémoires de l'Académie Royale des Sciences et Belles-Lettres de Bruxelles* 18:8.
- 702 White ER, Hasting A (2020) Seasonality in ecology: progress and prospects in theory. *Ecol*  
703 *Complex* 44:100867. <https://doi.org/10.1016/j.ecocom.2020.100867>
- 704 World Wildlife Fund (WWF) (2018) *Living planet report – 2018: aiming higher*. Grooten M,  
705 Almond REA (eds). World Wildlife Fund, Gland, Switzerland
- 706 Wysham DB, Hastings A (2008) Sudden shifts in ecological systems: intermittency and  
707 transients in the coupled Ricker population model. *Bull Math Biol* 70:1013-1031.  
708 <https://doi.org/10.1007/s11538-007-9288-8>  
709

710 **Figure Captions**

711 Figure 1. Population dynamics generated from a bi-seasonal Ricker model with season-specific  
712 habitat loss. Each generation is comprised of two counts: non-breeding population abundance  
713 (i.e., the number of individuals at the start of the non-breeding period; peaks), and breeding  
714 population abundance (i.e., the number of potential breeders at the start of the breeding period;  
715 troughs). The bi-seasonal time series includes two time-steps per generation. Replicate  
716 populations were simulated under control (no habitat loss conditions) for 20 generations while  
717 they grew toward carrying capacity (shaded grey region). In subsequent generations, season-  
718 specific habitat loss was simulated at 0% (control; a, d, g), 2%, 5%, 10%, 20%, or 25% per  
719 generation in either the breeding (b, e, h) or non-breeding period (c, f, i), under three different  
720 density dependence scenarios. (See *Model simulations* in *Methods*.) Sample size = 25 replicates  
721 per treatment.

722 Figure 2. Response of *per capita* reproduction to season-specific habitat loss with varying  
723 strengths of density dependence. In each generation, *per capita* reproduction was calculated as  
724 the number of offspring divided by the number of breeders. All replicates were simulated under  
725 control (no habitat loss conditions) for 20 generations while they grew toward carrying capacity  
726 (shaded grey region). In subsequent generations, season-specific habitat loss was simulated at  
727 0% (control; a, d, g), 2%, 5%, 10%, 20%, or 25% per generation in either the breeding (b, e, h)  
728 or non-breeding period (c, f, i), under three different density dependence scenarios. (See *Model*  
729 *simulations* in *Methods*.) Sample size = 25 simulations per treatment.

730 Figure 3. Response of non-breeding survival to season-specific habitat with varying strengths of  
731 density dependence. In each generation, non-breeding survival was calculated as the number of  
732 individuals at the end of the non-breeding period divided by the number initial non-breeding  
733 abundance (i.e., the proportion of individuals who survived through the non-breeding period).  
734 All replicates were simulated under control (no habitat loss conditions) for 20 generations while  
735 they grew toward carrying capacity (shaded grey region). In subsequent generations, season-  
736 specific habitat loss was simulated at 0% (control; a, d, g), 2%, 5%, 10%, 20%, or 25% per  
737 generation in either the breeding (b, e, h) or non-breeding period (c, f, i), under three different

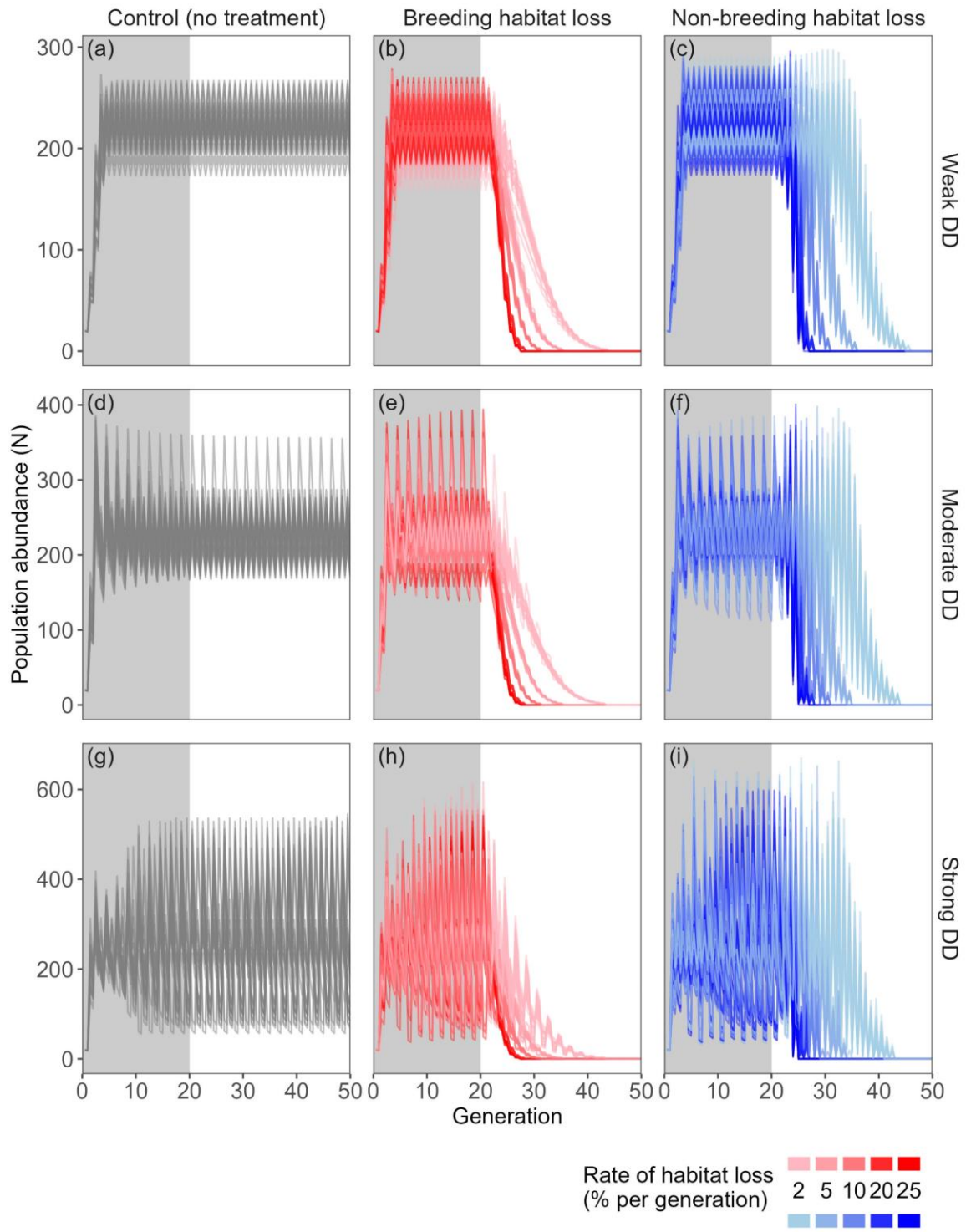
738 density dependence scenarios. (See *Model simulations* in *Methods*.) Sample size = 25  
739 simulations per treatment.

740 Figure 4. Rate of habitat loss, strength of density dependence, and the timing of population  
741 collapse with season-specific habitat loss. To explore how the strength of density dependence  
742 influences the timing of population collapse, we parameterized our bi-seasonal Ricker model  
743 under three different theoretical scenarios of density dependence and using the experimental  
744 parameters obtained from our seasonal populations of *Drosophila* (see *Model simulations* in  
745 *Methods*). The time to extinction was calculated as the number of generations of season-specific  
746 habitat loss at a particular rate before the populations collapsed, excluding the 20 generations of  
747 ‘pre-treatment’ in which populations were simulated under control conditions.

748 Figure 5. Effect of changing the strength of (a) non-breeding and (b) breeding density  
749 dependence for simulations of 10% non-breeding habitat loss. To explore the effect of density-  
750 dependence on time to extinction with non-breeding habitat loss, we systemically varied the  
751 strength of density dependence in either the breeding or non-breeding period, while holding  
752 density dependence constant in the other period (e.g., by setting breeding density dependence as  
753 moderate and vary the strength of non-breeding density dependence; see *Relative strength of*  
754 *density dependence* in *Methods*). Single, deterministic model runs were conducted for each  
755 pairwise combination of strengths of breeding and non-breeding density dependence. Extinction  
756 time was determined by performing a single iteration of the non-breeding habitat loss model with  
757 each combination of breeding and non-breeding strengths of density dependence.

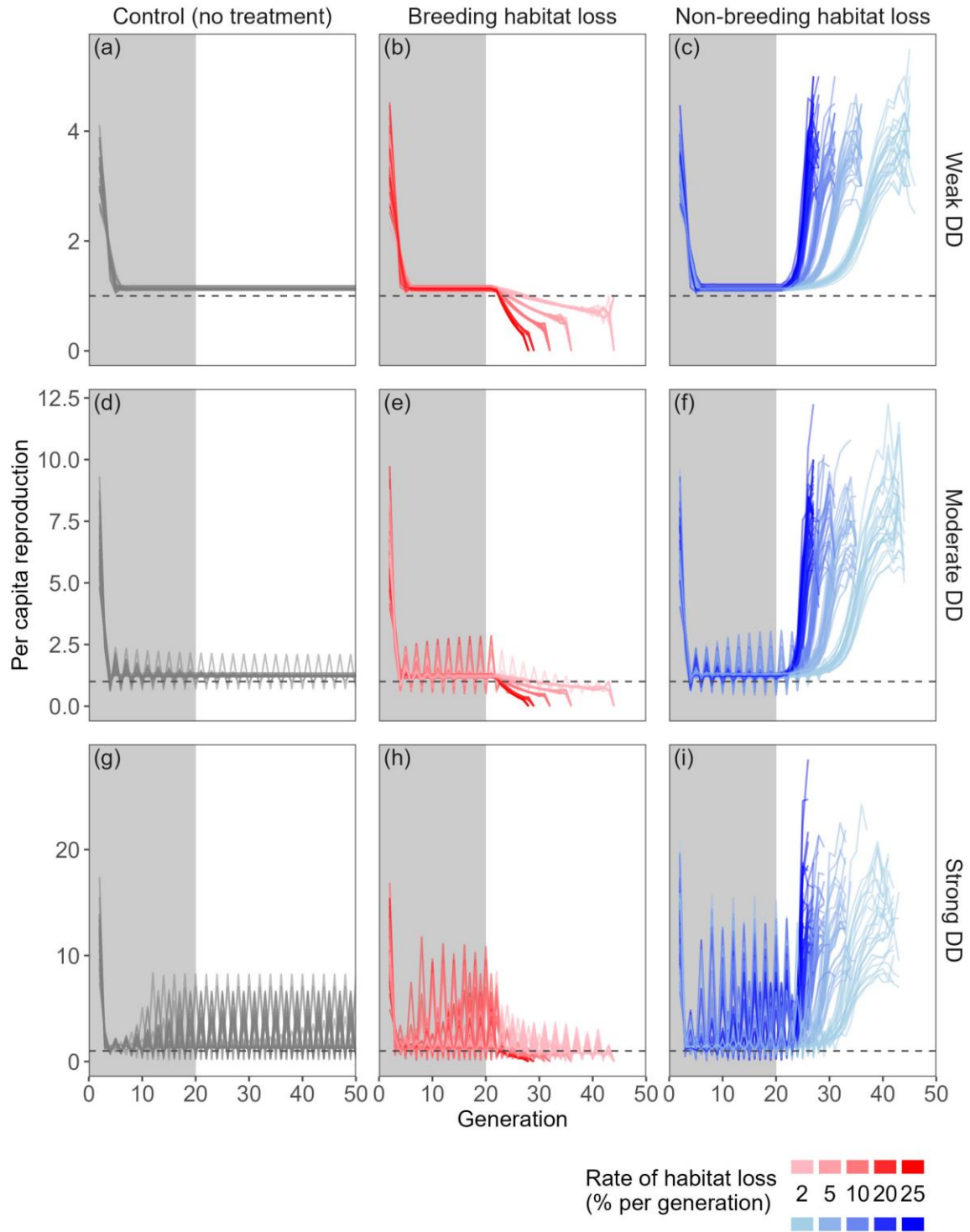
758 **Figures**

759 Figure 1.



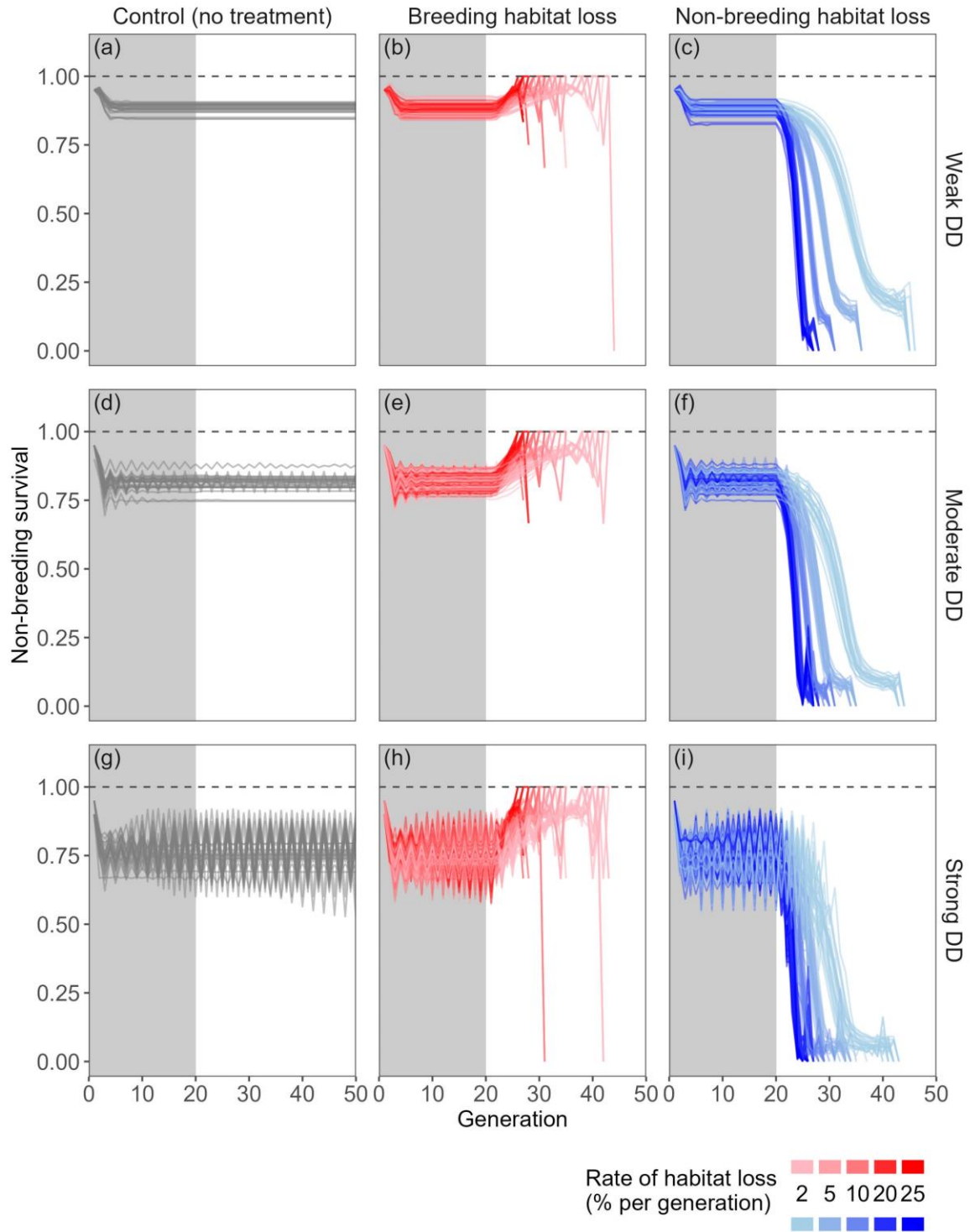
760

761 Figure 2.



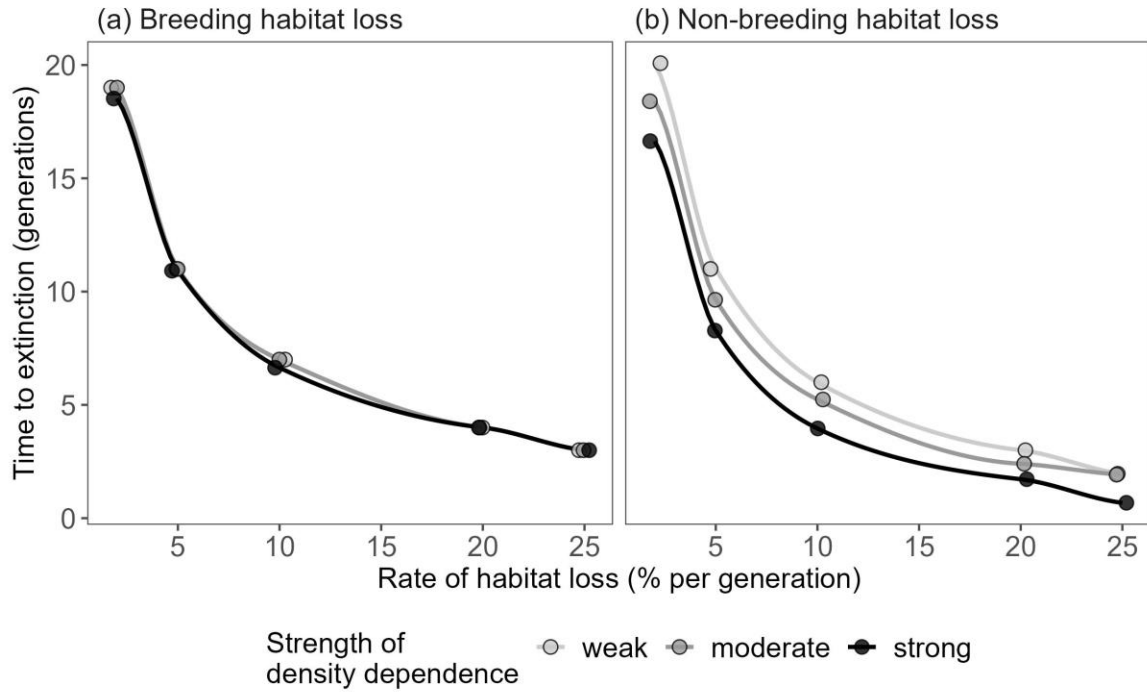
762

763 Figure 3.



764

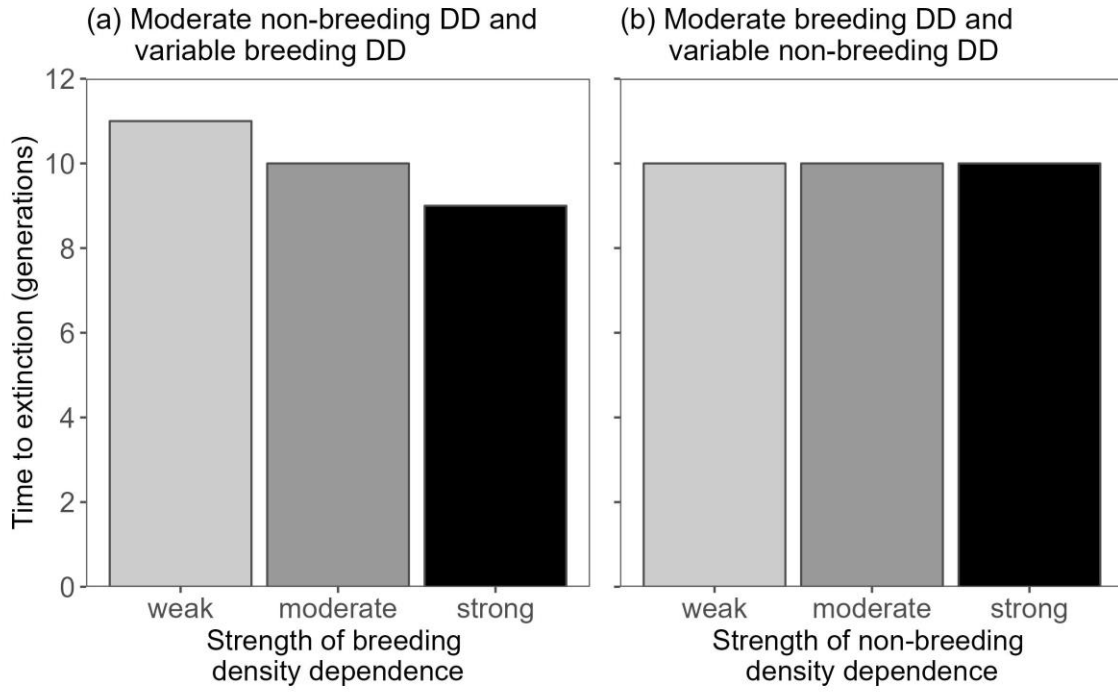
765 Figure 4.



766



767 Figure 5.



768